電解質陶瓷與電極之高溫界面反應研究 (2/2)

Study on the High Temperature Interfacial Reactions of Electrolyte Ceramics with Electrodes (2/2)

計畫編號: NSC 90-2216-E-002-028
執行期間:90/08/01~91/07/31

主持人：韋文誠 研究助理：楊志忠、王聖璋
國立台灣大學材料科學與工程學系暨研究所

摘要

本研究使用刮刀成形與網印技術，製備氧化釔安定化氧化鋯固態電解質與鑭鍶錳氧化物層狀試樣。試樣於 1000°C **至** 1400°C **空氣氣氛下共燒，持溫時間為** 1 **至** 120 **小時。經共燒後之試樣再於** 1000°C **作持溫** 1000 **小時的長時間熱處理。利用** X **光繞射儀、掃描式與分析式電子顯微鏡附屬能量散佈儀，來觀察與分析其微結構的變化與二次相的生成。實驗結果顯示，於** 1400°C **共燒初期，鑭鍶錳氧化物電極與氧化釔安定化氧化鋯電解質的相互擴散，造成界面處之氧化鋯形成一寬度約為** 70 nm **的非晶質區域。二次相鋯酸鑭與鋯酸鍶於此非晶質化的擴散層內，開始成核並遵循擴散控制機制成長。當提高共燒溫度與增長持溫時間，由於二次相的生成，使得三相界面處的孔隙率大幅減少，降低電化學可反應位置的數目。控制二次相的生成機制經確認為錳離子，反應擴散活化能為** 78 kJ/mol**，該值接近二次相生成的反應常數之活化能** (111 kJ/mol)**。此外，錳離子的擴散亦促使界面處之氧化鋯晶粒的成長；空缺擴散機制可能導致一寬度約為** 10 μm **的孔洞空乏區的形成。原先經** 1400°C**、**1 **小時共燒所形成的非晶質擴散層，再經由** 1000°C**、**1000 **小時的熱處理後，研究結果顯示無二次相的生成且界面處的氧化鋯會再結晶，此暗示當操作溫度低於** 1000°C **時可避免二次相的生成。**

關鍵字:**氧化釔安定化氧化鋯、鑭鍶錳氧化物、固態氧化物燃料電池、反應動力學**

ABSTRACT

The reaction kinetics between 8 mol% yttria-stabilized zirconia (YSZ) and 30 mol% Sr-doped Lanthanum Manganite ($La_{0.65}Sr_{0.30}MnO_3$, LSM) with A-site deficiency for the application of planar Solid Oxide Fuel Cells (SOFCs) were investigated. YSZ was fabricated by tape casting and then coated with a layer of LSM by screen-printing. The LSM/YSZ green tapes were co-fired from 1000°C to 1400°C for 1 h to 120 h and then annealed at 1000°C for up to 1000 h. The results showed that the inter-diffusion of cations between YSZ and LSM caused the amorphourization of YSZ after co-firing at 1400°C/1 h. $La_2Zr_2O_7$ (LZ) or $SrZrO_3$ (SZ) nuclei within the amorphous diffusion zone with vermicular features near the interface were observed after co-firing at 1400°C/1 h. The number of porosity at triple phase boundary (TPB) decreases significantly with increasing co-firing conditions. The transition of secondary phase changes from LZ to SZ with increasing co-firing temperature. The controlled reaction was confirmed to be the diffusion of Mn cations. The activation energy of Mn diffusion was 78 kJ/mol, close to that (111 kJ/mol) of rate constant. Moreover, the diffusion of cations (mainly Mn) from LSM to YSZ also enhances the grain growth of YSZ. The formation of pore-free zone (PFZ) of YSZ next to LSM was found and could be induced by vacancy diffusion mechanism. No formation of secondary phase can be found after annealing at 1000°C/1000 h, implying the interface is stable without the formation of secondary phases at the operation temperatures (≤ 1000°C).

Keywords: YSZ, LSM, SOFC, and Reaction kinetics

1. Introduction

8 mol% yttria-stabilized zirconia (YSZ) and strontium-doped lanthanum manganite (LSM) are the most commonly used solid electrolyte and cathode material, respectively, for solid oxide fuel cells (SOFCs). From the viewpoint of long-term stability of LSM/YSZ interfaces, the formation of secondary phases remains the biggest issue concerning the processing temperature and operation temperature. Literatures [1,2] have reported the formation of secondary phases when YSZ solid electrolyte contacts with LSM cathode material. $La_2Zr_2O_7$ (LZ) and $SrZrO_3$ (SZ) are the two reaction products for the combination with a low Sr content (x <0.3). However, only SZ becomes the dominant product for the case with a high Sr content (x > 0.3). The electrical conductivity of both zirconates is far lower than that of YSZ, leading to the degradation of energy conversion efficiency of SOFC. [3] Besides, it is reported that no chemical reaction occurs for $La_{1-x}Sr_xMnO_3$ with Sr substitution in the range of $0.2 \le Sr \le 0.4$ after annealing at 1400°C for 200 h. However, the microstructure, inter-diffusion of ions and kinetics of all interfacial reactions, if ever existing, with respect to co-firing and annealing conditions have not been determined yet.

In order to investigate the formation of secondary phases between YSZ and LSM in planar SOFC, a simplified model system, consisting of YSZ solid electrolyte fabricated by tape casting and then coated with the cathode material $La_{0.65}Sr_{0.30}MnO_3$ (LSM) by screen-printing, is demonstrated in the present work. After co-firing, the sintered LSM/YSZ specimens were annealed at temperatures between 1000°C and 1400°C for different soaking time. The results of the formation of secondary phases, microstructure and reaction kinetics were investigated with regard to processing conditions.

2. Experimental Procedures

8 mol% YSZ powder (TZ-8Y, Tosoh TZ-8Y, Japan) was used to prepare the YSZ slurries. A toluene/ethanol mixture was used as the solvent for the YSZ slurry preparation. YSZ slurries were cast by using a tape caster with two doctor blades on a silicone coated PET carrier tape (Hostaphan, Hoechst AG, Germany). YSZ green tapes coated with LSM pastes by screen-printing were then laminated by thermocompression (LA 4.5, Buerkle, Germany) at a pressure of 20 MPa and held at 70°C for 10 min. After lamination, the LSM/YSZ laminates were co-fired between 1000°C and 1400°C for 1 h in air furnace. Moreover, co-firing conditions such as 48 h at 1400°C are used in order to accelerate the reaction kinetics between LSM and YSZ. The sintered LSM/YSZ specimens were then annealed at 1000°C for up to 1000 h.

The formation of secondary phases was determined by X-ray diffractometry (PW 1710, Philips Instrument, Netherlands). The microstructures of LSM/YSZ specimens were examined by scanning electron microscopy (XL30 and Leo 1530, Philips, Netherlands), transmission electron microscopy (100 CXII, JEOL Co., Japan), and analytical electron microscopy (Tecnai 300 FE-TEM, Philips Co., Netherlands) equipped with EDS (DX4, EDAX Corp., USA). Moreover, the LSM/YSZ specimens was tilted to edge-on conditions and faced the EDS detector prior the EDS measurement so that the width of reaction layers was precisely observed and analyzed. In order to reduce the spurious effects such as absorption and beam broadening against precise and reliable composition measurement, the EDS microanalysis of all cations was performed on the LSM/YSZ interface, parallel to the direction of thickness fringe and normal to the interface of LSM/YSZ.

3. Results and Discussion

(1) Formation of Secondary Phases

Fig. 1 shows a series of XRD results of LSM/YSZ specimens, which were co-fired at 1400°C for 1 h to 48 h. The results indicate that no detectable secondary phases can be found after co-firing at 1400°C for 1 h, as shown in Fig. 1(a). However, very minor SZ and LZ phases are formed after co-firing at 1400°C for 10 h or longer, as shown in Figs. 1(b)-(c). The formation of SZ and LZ is consistent with those reported in literatures. [1]

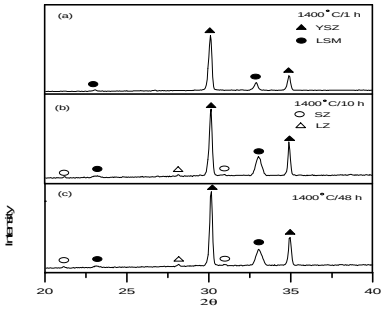

Fig. 1 XRD spectra of LSM/YSZ specimens, co-fired at 1400°C for (a) 1 h, (b) 10 h, and (c) 48 h.

Fig. 2 shows correspondent SEM microstructures of the LSM/YSZ specimens in Fig. 1. LSM is well attached to the YSZ and the interface between LSM and YSZ is clean when co-firing at 1400°C for 1-10 h, as shown in Figs. 2. However, two reaction layers, consisting of SZ and LZ in the range of 3-4 μm thick, were found after co-firing for 48 h. The morphology change at triple phase boundary with increasing holding time is significant. Obviously, LSM/YSZ specimens, co-fired at 1400°C for 10 h and longer, show a decrease in number, and growth in the size of porosity at triple phase boundary partially owing to the formation of secondary phases.

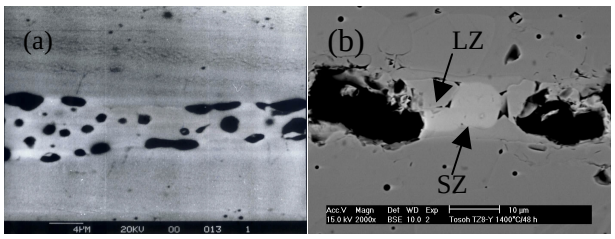

Fig. 2 The SEM microstructures of LSM/YSZ specimens, co-fired at 1400°C for (a) 1 h and (b) 48 h. Reaction products are found after co-firing at 1400°C for 48 h.

Fig. 3 shows the TEM micrographs, diffraction pattern, and EDS microanalysis of a LSM/YSZ specimen, co-fired at 1400°C for 1 h. The images show the interface consisted of YSZ and LSM crystals in a thickness of 30-80 nm, where a corrugated diffusion zone, mainly consisting of cubic YSZ partially substituted with Mn, La, and Sr is formed. Fig. 3(b) shows the vermicular structure in the diffusion zone, probably due to the amorphourization of cubic fluorite YSZ. Some of the nano-sized crystals, either SZ or LZ in the sizes of 10 nm, are found in the zone. The diffraction pattern of this diffusion zone, as shown in Fig. 3(c), is also composed of amorphous ring, which could be contributed from the amorphous phase. But the YSZ phase just behind this amorphous zone shows well crystallinity, as shown in Fig. 3(c).

Moreover, the concentration profile of a LSM/YSZ specimen as a function of diffusion depth is shown in Fig. 3(d). The concentration of Y and Zr diffused from the amorphous zone across the interface to LSM decreases rapidly. It is speculated that the formation of the diffusion zone basically proceeds due to the diffusion of Mn, La, and Sr to YSZ unidirectionally. The thickness of the amorphous diffusion zone is only in the range of 60-70 nm.

Fig. 4 shows SEM image and EDS analysis of a LSM/YSZ diffusion couple with Pt marker. Pt is a good marker candidate because of no reactivity with YSZ or LSM and its low vapor pressure (1.7×10^{-3} mm Hg) at 1400°C under oxidizing conditions. The LSM/Pt/YSZ diffusion couple was co-fired at 1400°C for 24 h. The SEM image shows that two reaction products are formed and identified as SZ and LZ. The thickness of SZ and LZ is about 2 μm and 5 μm, respectively. With the help of Pt

marker, the formation of secondary phases is determined to be mainly due to the diffusion of La, Sr and Mn to YSZ since the movement of Pt marker to LSM is found. Moreover, the concentration profiles of the cations as a function of diffusion distance are shown in Fig. 4(b). The EDS results indicate two compounds with the atomic ratio of 1:1 are formed. One is SZ and the other is LZ. For the convenience of explanation, the concentration of Zr, La and Sr in regions I and III is calibrated to 100 at%. The original concentration of Zr, La and Sr is 92 mol% (85.2 at%), 65 mol% (33.3 at%) and 30 mol% (15.4 at%), respectively. Minor amount of La, Sr and Mn in YSZ is found but no Zr or Y in LSM. Literatures [1] have reported that Mn diffuses faster than La and Sr cations to YSZ, resulting in La- and Sr-rich in LSM. As a consequence, perovskite phase is not stable, and transforms to La_2O_3 and SrO, and then may react with ZrO_2 to give LZ and SZ.

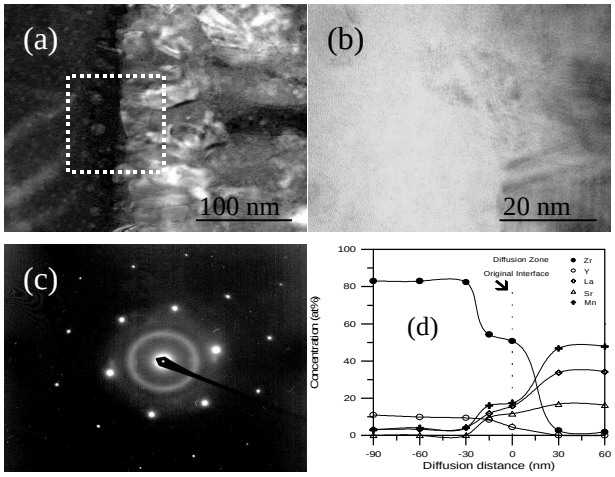

Fig. 3 LSM/YSZ specimen, co-fired at 1400°C/1 h, showing (a) TEM, (b) formation of SZ and LZ, (c) diffraction pattern, and (d) EDS microanalysis.

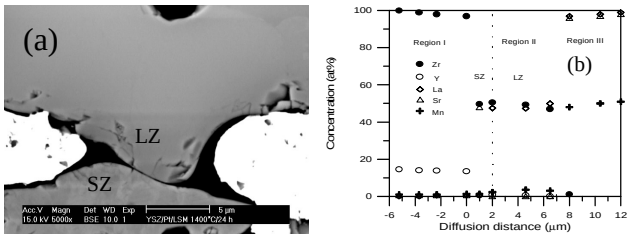

Fig. 4 SEM micrograph and concentration profile of a LSM/Pt/YSZ diffusion couple, showing (a) formation of secondary phases and (b) EDS results. The specimen was co-fired at 1400°C/24 h.

(2) Reaction Mechanism and Kinetics

Fig. 5 shows a series of SEM micrographs of LSM/YSZ specimens, co-fired from 1200°C to 1400°C for 36 h. The inter-diffusion between LSM and YSZ also becomes more pronounced while increasing temperature although the reaction products of those LSM/YSZ specimens, co-fired at 1200°C and 1300°C for 36 h, are not resolved by SEM. For LSM/YSZ specimens co-fired at 1400°C, the secondary phase can be clearly observed, as shown in Fig. 5(b).

The pore-free zone (PFZ) in the range of 10 μm is identified, as indicated in Fig. 5. The pores in the interior of YSZ move toward the interface, which acts as a vacancy sink during the pore migration. The formation of PFZ could be dominated by vacancy mechanism. Also, the pores coarsen greatly in LSM after co-firing at 1400°C for 36 h. The pore coarsening could be mainly both due to the accommodation of pores from YSZ and LSM. Therefore, the number of three-phase boundary is also greatly reduced. Moreover, the grain sizes of YSZ near the interface are bigger than those in the YSZ matrix grains. It is found in our work that the grain growth of YSZ is mainly due to the diffusion of Mn cation, which will be shown and discussed in detail again in Fig. 7.

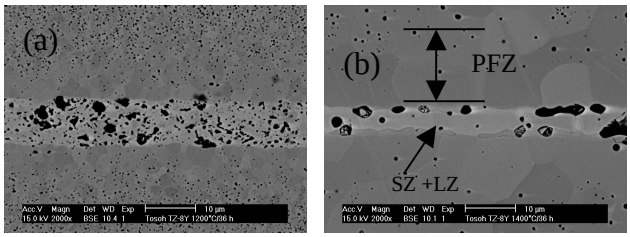

Fig. 5 SEM micrographs of LSM/YSZ specimens, which were co-fired at (a) 1200°C, (b) 1400°C for 36 h, respectively.

Fig. 6(a) shows the relationship between thickness of secondary phases and time of LSM/YSZ specimens, which were co-fired at 1000°C to 1400°C for up to 120 h. The diffusion coefficients and reaction constants as a function of temperature of LSM/YSZ specimens are shown in Fig. 6(b). By the combination of Arrhenius equation and parabolic law, the controlled reaction mechanism of the formation of secondary phases can be determined. The result shows that Mn cation has the fastest diffusion coefficient and its activation energy for diffusion is 78 kJ/mol, is close to that (111 kJ/mol) of reaction constant *k*. In other words, the chemical reaction of the formation of secondary phases is controlled by the diffusion of Mn.

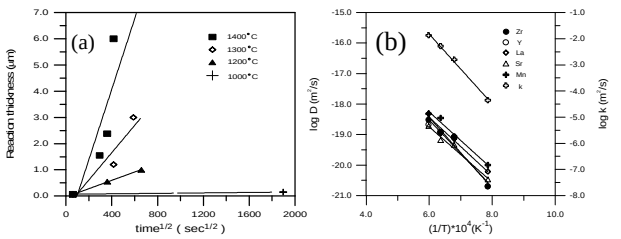

Fig. 6(a) Reaction constant as a function of $t^{1/2}$ and (b) Arrhenius plot of D versus 1/T for LSM/YSZ specimens.

A reaction mechanism of the formation of secondary phases involving several steps is proposed: (1) Diffusion of cations from LSM (mainly Mn) leads to the amorphourization of cubic fluorite structure of YSZ; (2)

Mn cation diffuses faster among five cationic species due to the greatest diffusion coefficient in the amorphous diffusion zone; (3) A-site becomes rich in La and Sr due to faster Mn migration; (4) formation of excessive La_2O_3 and SrO, leading to the formation of LZ and SZ; (5) Transition of secondary phases from LZ to SZ takes places as the amount of La_2O_3 is too low to react with ZrO_2 to give LZ and (6) growth of secondary phase toward YSZ unidirectionally.

(3) Long-Term Stability Test at 1000îC

Fig. 7 shows the SEM image and EDS analysis of a LSM/YSZ specimen, annealed at 1000°C for 120 h. The exaggerated grain growth of YSZ was ascribed to both the diffusion of Mn and temperature effect. At higher temperatures, it is reasonable that the grain growth takes place as long as the time is sufficient. However, the effect of temperature at 1000°C on the grain growth could be ignored, the grain growth of YSZ remains sluggish at the temperature lower than 1100°C. [4] Kim *et al.* [5] reported that the solid solubility of Mn_2O_3 is 12 mol% at 1400°C in YSZ. The grain size of YSZ increases with increasing the Mn_2O_3 content within the solubility limit in YSZ. [5] Therefore, the diffusion of Mn to YSZ enhances the grain growth of YSZ and is consistent with the literature. Fig. 7(b) shows the semi-quantitative EDS results of a LSM/YSZ specimen, annealed at 1000°C for 120 h. The EDS result has confirmed the diffusion of Mn in larger quantity to YSZ while the diffusion of La and Sr is relatively low.

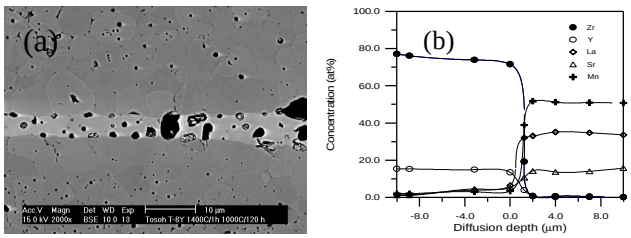

Fig. 7(a) SEM microstructures and (b) EDS data of LSM/YSZ specimens, which are co-fired at 1400°C/1 h and then annealed at 1000°C for 120 h.

Fig. 8 show the TEM micrograph and concentration profile of a LSM/YSZ specimen, co-fired at 1400°C/1 h and then annealed at 1000°C for 1000 h. The result shows that a crystalline diffusion layer of 100 nm is formed. The EDS microanalysis shows the diffusion of La, Sr and Mn to YSZ. The composition and structure of this nano-crystalline diffusion layer is consisted of cubic fluorite YSZ structure. The initially amorphous diffusion zone after co-firing at 1400°C/1 h, shown in Fig. 3, crystallizes under the specified condition. It is believed that the recrystallization of this diffusion zone may retard the further formation of secondary phases of SZ and LZ due to its slower diffusion rate in solid phase.

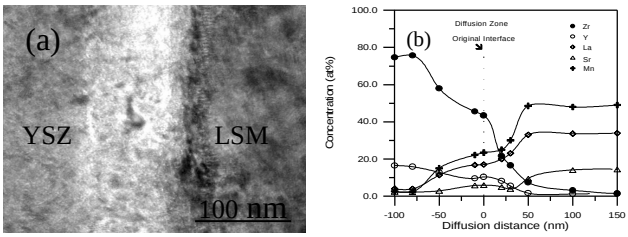

Fig. 8 LSM/YSZ specimen, co-fired at 1400°C/1 h and then annealed at 1000°C for 1000 h shows (a) TEM micrograph and (b) concentration profile.

4. Conclusions

The conclusions of this work are as follows:

1. The diffusion of La, Sr and Mn has caused the amorphourization of YSZ and the thickness of this amorphous diffusion zone is only about 70 nm. Two reaction products, identified as SZ and LZ, are formed.
2. The number of porosity at the three-phase boundary is greatly reduced because of the formation of secondary phases. LZ and SZ are the dominant phases in a low and high Sr substitution for LSM/YSZ systems.
3. A reaction mechanism of the formation of LZ and SZ involving a series of steps is proposed. The results show that the formation of secondary phases is controlled by the diffusion of Mn cations. The activation energy of Mn diffusion is 78 kJ/mol, close to that (111 kJ/mol) of reaction constant.
4. The initially amorphous diffusion zone after co-firing at 1400°C/1 h crystallizes when annealing at 1000°C/1000 h, which may prevent the further nucleation and growth of LZ. Moreover, a pore-free zone (PFZ) in the range of 10 μm was formed. The movement of pores from YSZ leads to the formation of PFZ and could be enhanced and dominated by the vacancy mechanism.

Acknowledgements

The authors acknowledge the financial supports under the contract NSC 90-2216-E-002-028.

Reference

1. H. Taimatsu, K. Wada and H. Kaneko, J. Am. Ceram. Soc., 75 [2] pp. 401-05 (1992)
2. S. Faaland, M.-A. Einarsrud, K. Wiik and T. Grande, J. Mater. Sci., 34, pp. 957-66 (1999)
3. Y. C. Hsiao and J. R. Selman, Solid State Ionics, 98, pp. 33-38 (1997)
4. D. J. Chen and M. J. Mayo, J. Am. Ceram. Soc., 79 [4], pp. 906-12 (1996)
5. J. H. Kim and G. M. Choi, Solid State Ionics, 130, pp. 157-68 (2000)